Unimolecular reaction dynamics from kinetic energy release distributions. III. A comparative study of the halogenobenzene cations

P. Urbain, B. Leyh, F. Remacle, A. J. Lorquet, R. Flammang, and J. C. Lorquet

Citation: The Journal of Chemical Physics **110**, 2911 (1999); doi: 10.1063/1.477934
View online: http://dx.doi.org/10.1063/1.477934
View Table of Contents: http://scitation.aip.org/content/aip/journal/jcp/110/6?ver=pdfcov
Published by the AIP Publishing

Unimolecular reaction dynamics from kinetic energy release distributions. III. A comparative study of the halogenobenzene cations

P. Urbain, B. Leyh, F. Remacle, and A. J. Lorquet
Département de Chimie, Université de Liège, Sart-Tilman, B-4000 Liège 1, Belgium

R. Flammang
Département de Chimie Organique, Université de Mons-Hainaut, 19, avenue Maistriau, 7000 Mons, Belgium

J. C. Lorquet
Département de Chimie, Université de Liège, Sart-Tilman, B-4000 Liège 1, Belgium

(Received 26 May 1998; accepted 4 November 1998)

The translational kinetic energy release distribution (KERD) in the halogen loss reaction of the chloro-, bromo-, and iodobenzene cations has been experimentally determined in the microsecond time scale and theoretically analyzed by the maximum entropy method. The KERD is constrained by the square root of the translational energy, i.e., by the momentum gap law. This can be understood in terms of quantum-mechanical resonances controlled by a matrix element involving a localized bound state and a rapidly oscillating continuum wave function, as in the case of a vibrational predissociation process. The energy partitioning between the reaction coordinate and the set of the remaining coordinates is nearly statistical, but not quite: less translational energy is channeled into the reaction coordinate than the statistical estimate. The measured entropy deficiency leads to values of the order of 80% for the fraction of phase space sampled by the pair of fragments with respect to the statistical value. In the case of the dissociation of the chlorobenzene ion, it is necessary to take into account a second process which corresponds to the formation of the chlorine atom in the excited electronic state $^2P_{1/2}$ in addition to the ground state $^2P_{3/2}$. The observations are compatible with the presence of a small barrier (of the order of 0.12 eV) along the reaction path connecting the $\tilde{D}\,^2A_1$ state of $C_6H_5Cl^+$ to the $Cl(^2P_{1/2})+C_6H_5^+(\tilde{X}\,^1A_1)$ asymptote. © *1999 American Institute of Physics.* [S0021-9606(99)00906-X]

I. INTRODUCTION

Does a unimolecular chemical reaction proceed statistically or is it possible to favor a chosen reaction channel by selectively exciting some internal modes? This central question in chemical physics has been for about 60 years an incentive to the development of a variety of experimental techniques and theoretical methods.

Mass spectrometric experimentation and modeling have contributed to this debate. The vast majority of unimolecular dissociations involving ions have been interpreted as statistical processes. Ultrafast internal conversions and rapid intramolecular vibrational energy redistribution (IVR) are assumed to be completed before the dissociation step. Stated in other terms, phase space is expected to be sampled in a uniform way. Statistical models[1–4] have been developed[5–12] to study unimolecular rate constants: variational transition state theory, transition state switching model, phase space theory, orbiting transition state theory, and statistical adiabatic channel model.

However, product energy distributions are much more sensitive to any deviation from a pure statistical situation.[3,13,14] Compared with the rate constants, they provide us with complementary information, because they reveal the sampling of the phase space associated with the dissociation fragments.

In this paper, we adopt an approach based on the analysis, by the maximum entropy formalism,[15–20] of experimental fragment energy distributions for ionic unimolecular dissociations. More precisely, we measure by sector tandem mass spectrometry, under collision-free conditions, the translational kinetic energy released to the dissociation fragments in the metastable time window ($10^{-6}-10^{-5}$ s). As a consequence of this time selection, the dissociating parent ions are characterized by a relatively wide (about 0.5 eV) bell-shaped internal energy distribution, centered at a given energy, hereafter denoted E_S. The measured kinetic energy release distribution is then, in a second step, compared with the corresponding purely statistical estimate, called the prior distribution, for which all exit channels at a given total energy are considered to be equiprobable. From the observed deviations from this microcanonical equilibrium, the maximum entropy method makes it possible to infer (i) the nature of the dynamical constraints which are responsible for the deviations and (ii) the fraction of phase space which is effectively sampled.

The set of reactions chosen for the present work is the loss of the halogen atom from ionized halogenobenzene cations ($C_6H_5X^+$ with X=Cl, Br, I), which have previously received extensive attention.[21–38] A first account dealing only with the bromobenzene case has already been published.[39] As far as bromo- and iodobenzene are con-

cerned, these studies have concluded that the dissociation proceeds statistically, via an extremely loose transition state. However, in the case of the loss of Cl from $C_6H_5Cl^+$, the data of Pratt and Chupka[24] and of Yim and Kim[37] were best accounted for by a model involving a nontotally loose transition state. As will appear in the present paper, the latter dissociation turns out to be a much more challenging problem.

Furthermore, although the parent ion internal energy distributions are quite wide, as previously mentioned, some control on the time selection and thus on the average internal energy is nevertheless possible by working at different ion source accelerating voltages or by using different field-free regions. In the present work, we could shift the internal energy distribution by about 0.15–0.2 eV. This shift has been instrumental for the unambiguous identification of the dynamical constraint involved in the dissociation process. In principle, it makes it also possible to investigate how phase space sampling varies with internal energy.

The paper is organized as follows. The experimental method is described briefly in Sec. II and the results are presented in Sec. III. Next, the salient points of the maximum entropy formalism relevant to the present experimental framework are reviewed in Sec. IV. The dissociations of the bromo- and iodobenzene ions show a very similar behavior and are discussed together in Sec. V. The influence of the internal energy on the efficiency of phase space sampling is studied in Sec. VI. Section VII is devoted to the more complex case of chlorobenzene. Concluding remarks are presented in Sec. VIII.

II. EXPERIMENT

A. Kinetic energy release distributions

Our spectra have been recorded with a forward geometry two-sector (AEI-MS9) mass spectrometer, i.e., an instrument where an electrostatic analyzer is followed by a magnetic sector. As we are interested in metastable dissociations, it is very desirable to carry out experiments with various time windows and thus with various internal energy contents of the dissociating ions. For this purpose, dissociations taking place in both the first field-free region (between the ion source exit slit and the electrostatic analyzer) and the second field-free region (between the electrostatic analyzer and the magnet) and in different accelerating voltage ranges have been monitored. Either the accelerating voltage scan method[40] (V-scan) or the linked scanning of the electrostatic analyzer and the magnet at constant B^2/E ratio[41] were used to record fragment ion kinetic energy spectra for dissociations taking place in the first field-free region. Magnet scanning[42] was used to investigate dissociations in the second field-free region.

The translational kinetic energy released to the fragments during a dissociation brings about a signal broadening which is detected in the corresponding ion kinetic energy spectrum measured in the laboratory reference frame. From a physical point of view, one is interested in the kinetic energy released in the center-of-mass frame. When instrumental broadening as well as discrimination in the direction perpendicular to the ion flight path can be neglected, the KERD (in the center-of-mass frame), $\tilde{P}(\varepsilon)$, can be obtained by differentiation of the measured ion kinetic energy spectrum followed by a transformation of variables from the laboratory coordinates to the center-of-mass coordinates.[43–45] Carrying out this differentiation either numerically or using the Holmes–Osborne procedure[43] led to no significant difference. In the decompositions investigated in this paper, the amount of kinetic energy released to the fragments in the laboratory frame is negligible ($<$50 eV) compared with the kinetic energy of the center of mass (a few keV, depending on the accelerating voltage), so that discrimination effects can be neglected. This eliminates the need to calculate explicitly the basis functions describing the response of the kinetic energy analyzer to a hypothetical kinetic energy release distribution expressed by a Dirac delta function. The electrostatic analyzer exit slit (β-slit) has been closed to 0.25 mm to reach an energy resolution $\Delta E/E$ of 10^{-3}, which makes any deconvolution procedure unnecessary.

Accelerating voltage scan spectra have been recorded for fragment ion translational energies ranging between 1 and 5 keV (in the laboratory frame). B^2/E as well as magnet scan spectra have been measured with an accelerating voltage equal to 8 kV. The following ion source conditions were applied. Trap current: 30μA. Electron energy: 70 eV, except for the magnet scan spectra for which the electron energy has been reduced to 14.6 eV in order to eliminate overlap with more intense signals coming from fragment ions produced in the ion source. Ion source pressure (measured at an ion gauge located approximately 15 cm from the ionization chamber): 10^{-4} Pa. The pressure in the field-free regions was kept in the 10^{-6} Pa range, in order to avoid collision-induced dissociations. Chloro-, bromo-, and iodobenzene provided by Fluka (99.5% stated purity) were carefully degassed but otherwise used without further purification.

B. Internal energy distribution of the metastable parent ions

The dissociations sampled in our experiments correspond to a time window defined by the entry and exit times, τ_1 and τ_2, in the field-free region. These times can be easily calculated using elementary physics based on the spectrometer geometry parameters and operating conditions. Accordingly, the measured kinetic energy release distributions do not correspond to a well defined energy but to a distribution of internal energies, $T(E)$. Indeed, the corresponding collection efficiency T depends on the rate constant which, in turn, depends on the internal energy E:

$$T[k(E)] = B[\exp(-k(E)\tau_1) - \exp(-k(E)\tau_2)]. \quad (2.1)$$

Throughout this paper, the internal energy, E, is expressed with respect to the dissociation asymptote. B is a normalization constant. The functions $k(E)$ have been experimentally determined by various authors.[21–31,33,34,36,37] Their energy dependence in the domain covered by $T(E)$ has been fitted to the following empirical form using the different experimental values available from the literature:

$$k(E) = k_{\text{opt}}\left(\frac{E}{E_s}\right)^{\nu}, \quad (2.2)$$

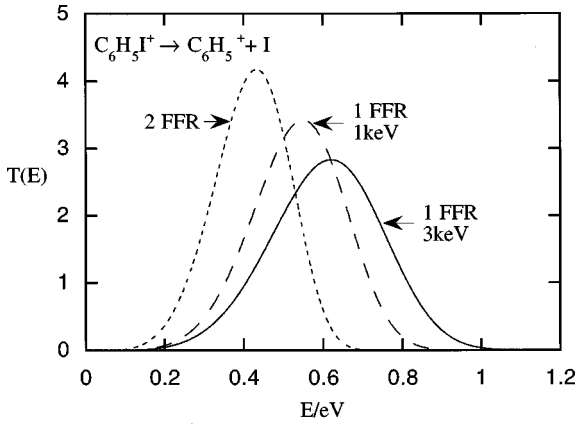

FIG. 1. Collection efficiency $T(E)$ [Eq. (2.1)] for the metastable dissociation $C_6H_5I^+ \rightarrow C_6H_5^+ + I$ taking place in the two field-free regions of the AEI-MS9 mass spectrometer under different experimental conditions defined in the figure.

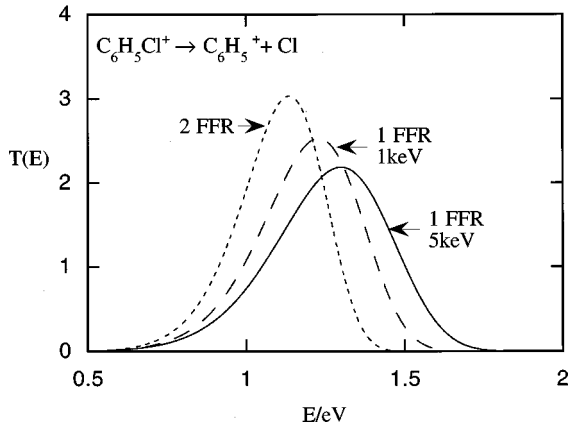

FIG. 2. Collection efficiency $T(E)$ [Eq. (2.1)] for the metastable dissociation $C_6H_5Cl^+ \rightarrow C_6H_5^+ + Cl$ taking place in the two field-free regions of the AEI-MS9 mass spectrometer under different experimental conditions defined in the figure.

where k_{opt} is the value of the rate constant at the energy E_S at which $T(E)$ reaches its maximum.

The excitation process is by electronic impact and thus inherently nonselective. The experimental data are therefore the result of an average over the range of internal energies defined by $T(E)$. The measured distribution of translational energies $\tilde{P}(\varepsilon)$ is given by:

$$\tilde{P}(\varepsilon) = \int_{\varepsilon}^{\infty} T(E) P(\varepsilon|E) dE, \tag{2.3}$$

where $P(\varepsilon|E)$ is the translational kinetic energy release distribution at a given internal energy E.

Figures 1 and 2 show the $T(E)$ functions obtained under three different sets of experimental conditions, corresponding to three different time windows, for the loss of I or Cl from ionized iodobenzene or chlorobenzene, respectively. These data illustrate the extent of the upward shift of $T(E)$ with decreasing lifetime. The values of k_{opt}, E_S, ν, τ_1 and τ_2 are summarized in Table I for the three halogenobenzenes.

III. RESULTS

The kinetic energy release distributions have been recorded under various experimental conditions corresponding to different internal energy distributions. In the first field-free region, we investigated the following processes using the V-scan technique. In some cases, the results have been checked by the B^2/E linked scanning method.

$$C_6H_5Cl^+ \rightarrow C_6H_5^+ (5 \text{ and } 1 \text{ keV}) + Cl,$$

$$C_6H_5Br^+ \rightarrow C_6H_5^+ (4 \text{ and } 1 \text{ keV}) + Br,$$

$$C_6H_5I^+ \rightarrow C_6H_5^+ (3 \text{ and } 1 \text{ keV}) + I.$$

These dissociations have also been all monitored in the second field-free region,

$$C_6H_5X^+ (8 \text{ keV}) \rightarrow C_6H_5^+ + X (X = I, Br, Cl).$$

As typical examples, the kinetic energy release distributions $\tilde{P}(\varepsilon)$ obtained for the dissociation of the iodobenzene cation in the first field-free region with a fragment ion kinetic energy of 1 and 3 keV (in the laboratory frame) are presented in Figs. 3 and 4. (Similar data for the bromobenzene ion can be found in Part II of this series.[39]) These results are averages of 12 distributions recorded over a period of one year. The values of the first few moments ($\langle\varepsilon\rangle$, $\langle\varepsilon^{1/2}\rangle$, and $\langle\varepsilon^2\rangle$) are presented in Table I. The average kinetic energies $\langle\varepsilon\rangle$ are in good agreement with the previous values obtained by Burgers and Holmes.[28] In particular, we confirm their slow variation with the internal energy.

IV. THE MAXIMUM ENTROPY METHOD

An analysis of a product state distribution by the maximum entropy method consists of comparing the actual, experimentally observed distribution $P(\varepsilon|E)$ with the prior distribution $P^0(\varepsilon|E)$ which serves as a reference.[15–20] The decisive advantage of this formalism is that its functional form relating the experimentally observed KERD to the prior distribution is not simply an empirical parametrization. It involves constraints which are related to observables and which, therefore, possess a physical significance. A different set of constraints implies a difference in the reaction mechanism.

The prior distribution is the least biased distribution, that is the most statistical distribution in phase space, where no dynamical effects have been included.[15–20] Its entropy is therefore maximal. This distribution is defined as that for which all quantum states at a given total energy are equiprobable, i.e., every group of product states that is energetically allowed is populated with a probability proportional to the number of quantum states of that group. Therefore, the only constraint that is included in the counting of the quantum states is the conservation of the total energy. The conservation of the total angular momentum is an additional general constraint (good constant of motion of the total Hamiltonian) that limits the number of final states that are accessible. However, the inclusion of the conservation of the total angular momentum requires a theoretical decision about the ''cutoff'' (one has to decide what the value of $J_{\max}$ is)[46]

TABLE I. Time window and most probable internal energy E_S, first moments of the KERDs, and values of λ_0, DS, and e^{-DS} for $E=E_S$ obtained for the different metastable decompositions investigated in this work. For first field-free region (1st FFR) experiments, the fragmentation translation energy in the laboratory frame is mentioned. Experiments in the second field-free region (2nd FFR) have been conducted with an accelerating voltage of 8 kV. The relative uncertainty on the average KER $\langle\varepsilon\rangle$ is estimated to be of the order of ±3%. The uncertainty on e^{-DS} is equal to ±0.03.

	$C_6H_5Cl^+\rightarrow C_6H_5^+ + Cl$			$C_6H_5Br^+\rightarrow C_6H_5^+ + Br$			$C_6H_5I^+\rightarrow C_6H_5^+ + I$		
	2nd FFR	1st FFR 1 kV	1st FFR 5 kV	2nd FFR	1st FFR 1 kV	1st FFR 4 kV	2nd FFR	1st FFR 1 kV	1st FFR 3 kV
τ_1 (μs)	9.89	4.16	1.53	11.75	4.16	1.74	13.35	4.16	2.00
τ_2 (μs)	13.3	8.22	3.35	15.80	8.22	3.77	17.95	8.22	4.34
E_S (eV)	1.13	1.23	1.30	0.67	0.75	0.85	0.47	0.55	0.62
k_{opt} (10^5 s^{-1})	0.863	1.68	4.3	0.73	1.68	3.8	0.64	1.68	3.3
ν	8.95	8.15	7.47	6.30	6.05	6.00	5.40	4.80	4.50
$\langle\varepsilon^{1/2}\rangle$ ($eV^{1/2}$)	0.269	0.275	0.269	0.219	0.221	0.221	0.196	0.194	0.206
$\langle\varepsilon\rangle$ (eV)	0.090	0.096	0.091	0.059	0.060	0.060	0.046	0.045	0.051
$\langle\varepsilon^2\rangle$ (eV^2)	0.0156	0.0183	0.0161	0.0069	0.0073	0.0069	0.0038	0.0037	0.0049
λ_1 ($eV^{-1/2}$)	5.1[a]	4.9[a]	6.0[a]	5.4	6.2	6.7	5.8	7.2	6.4
λ_0	−1.47[a]	−1.45[a]	−1.74[a]	−1.36	−1.56	−1.72	−1.33	−1.65	−1.55
DS	0.19[a]	0.19[a]	0.27[a]	0.16	0.22	0.26	0.15	0.24	0.21
e^{-DS}	0.83[a]	0.83[a]	0.76[a]	0.85	0.80	0.77	0.86	0.79	0.81

[a]Data corresponding to the main reaction channel of $C_6H_5Cl^+$.

and therefore an assumption about the dynamics. In the present work, following the point of view expressed in Ref. 17, we choose to retain for the prior distribution the least biased distribution without including the conservation of the total angular momentum. Moreover, since in the studied reactions the reduced mass along the reaction coordinate is sufficiently large to lead to high values of the orbital angular momentum, the discrepancy between the experimental and the prior distributions is not expected to be due to the constraint imposed by the conservation of the total angular momentum.[47]

The actual distribution $P(\varepsilon|E)$ measures the translational energy of the pair of fragments. Therefore, a definition of the prior distribution for translational states is needed. The three-dimensional density of translational states per unit volume and per unit energy[4,17,19,48] is, for an isotropic angular distribution,

$$\rho_T(\varepsilon)d\varepsilon = A_T\varepsilon^{1/2}d\varepsilon, \tag{4.1}$$

with

$$A_T = \mu^{3/2}/(2^{1/2}\pi^2h^3), \tag{4.2}$$

where μ is the reduced mass along the reaction coordinate.

At a given total energy E, the rovibrational density of states $N(E-\varepsilon)$ can be approximated by a continuous function. The prior distribution is therefore given by

$$P^0(\varepsilon|E) = A(E)\varepsilon^{1/2}N(E-\varepsilon), \tag{4.3}$$

where $A(E)$ is a normalization factor.

This functional form for the prior distribution is equivalent to that derived for the actual distribution in phase space theory[49] in the case of a loose complex bound by long-range polarizability forces.[50] The difference is one of methodology, i.e., we first get the functional form (4.3) by taking for the prior distribution the least biased one, without making any assumption on the form of the potential along the reaction coordinate or on the ''cutoff'' value of the total angular momentum. Then, in a second stage discussed below [Eqs. (4.4)

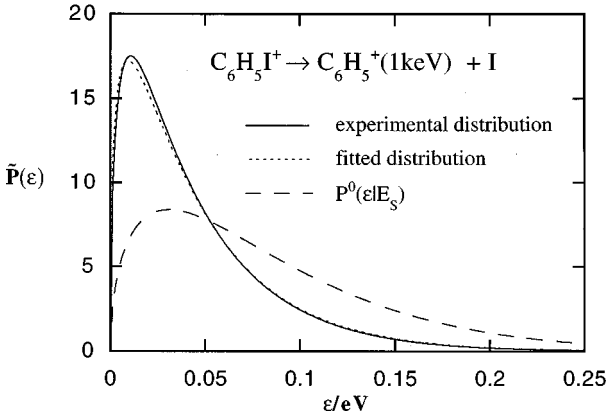

FIG. 3. Experimental (solid line) and fitted (dots) kinetic energy release distributions obtained for the metastable dissociation $C_6H_5I^+\rightarrow C_6H_5^+$ (1 keV)+I (first field-free region). The prior distribution [Eq. (4.3)] at $E=E_S$ is drawn in dashed lines.

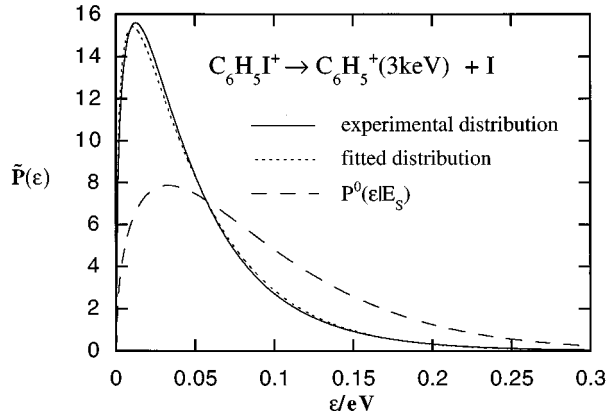

FIG. 4. Experimental (solid line) and fitted (dots) kinetic energy release distributions obtained for the metastable dissociation $C_6H_5I^+\rightarrow C_6H_5^+$ (3 keV)+I (first field-free region). The prior distribution [Eq. (4.3)] at $E=E_S$ is drawn in dashed lines.

and (5.1)], we parametrize the discrepancy between the actual (experimental) and the prior distributions using the maximum entropy formalism.

The rovibrational density of states, $N(E-\varepsilon)$, is generated by a Beyer–Swinehardt algorithm[2,4,51] where the rotational parameters and the vibrational frequencies have been calculated *ab initio* at the RHF/6-31G(d) level.[38,39] In the case of the chlorobenzene cation, a rovibronic density of states is calculated, because, as discussed in Sec. VII below, the Cl atom is assumed to be generated in both of its $^2P_{3/2}$ and $^2P_{1/2}$ electronic states.

In the second step of our analysis, we seek a quantitative parametrization of the discrepancy between the prior and the actual distributions. In the maximum entropy formalism,[16,17,19,20] the actual distribution is shown to be related to the prior distribution in the following way:

$$P(\varepsilon|E)=P^0(\varepsilon|E)\exp\left(-\lambda_0-\sum_{r=1}^{n}\lambda_r A_r\right), \tag{4.4}$$

where the quantities A_r are physical observables and the λ_r are the conjugated Lagrange parameters. The average values $\langle A_r\rangle$ of the observables A_r over the actual distribution $P(\varepsilon|E)$ are the constraints. $P(\varepsilon|E)$ in Eq. (4.4) is the unique normalized distribution that satisfies the n constraints $\langle A_r\rangle$ and that is otherwise of maximum entropy.

The entropy deficiency DS is the difference between the entropy of the prior distribution (denoted S^0) and that of the actual one (denoted S),

$$DS(E)=S^0(E)-S(E)=\int_0^E P(\varepsilon|E)\ln\left[\frac{P(\varepsilon|E)}{P^0(\varepsilon|E)}\right]d\varepsilon. \tag{4.5}$$

The entropy deficiency DS is always positive or equal to zero and the quantity e^{-DS} measures the fraction of phase space effectively sampled by the pair of fragments.[52,53]

V. THE DISSOCIATION OF THE BROMO AND IODOBENZENE CATIONS

For the unimolecular fragmentation of the $C_6H_5Br^+$ ion previously investigated,[39] very good least-squares fits led us to argue that the appropriate functional form involves a single constraint, viz., $\varepsilon^{1/2}$, so that Eq. (4.4) becomes

$$P(\varepsilon|E)=P^0(\varepsilon|E)\exp[-\lambda_0-\lambda_1\varepsilon^{1/2}]. \tag{5.1}$$

We emphasize that this conclusion concerning the nature of the informative constraint results not only from the quality of the individual fits but also from self-consistency checks based on the analysis of KERDs corresponding to different energy windows. The shape of the experimental distribution does not show any fine structure, so that a single constraint can be expected to generate a good fit, at least in the case of bromo- and iodobenzene. In principle, λ_1 depends on the internal energy. However, this energy dependence was neglected in the energy domain covered by a given transmission function (see Figs. 1 and 2). The average value of both ε and $\varepsilon^{1/2}$ were indeed observed (Table I) to be nearly the same in the different energy windows, a fact which is confirmed by independent measurements carried out by other authors.[28] The functional form (5.1) with energy independent Lagrange parameters, together with the averaging over the distribution of internal energies (2.3), was found to fit adequately all our data in the case of both the iodo- and bromobenzene ions. Figures 3 and 4 show the fits obtained for the $C_6H_5I^+$ ion in the first field-free region with a fragment ion kinetic energy of 1 and 3 keV in the laboratory frame. In the case of chlorobenzene, the functional form (5.1) involving a single constraint did not lead to satisfactory fits, as discussed in detail in Sec. VII.

As we now elaborate, the rationale for Eq. (5.1) is that the reaction can essentially be thought of as a vibrational predissociation. The definition of the latter term requires qualifications.[4] In the particular case of van der Waals complexes, the rate of decay associated with this process has been extensively studied. These complexes fragment in a very nonstatistical way and their rate constants are orders of magnitude slower than the statistical limit because the intramolecular energy redistribution is hindered by the frequency mismatch between the weak van der Waals bond and the stronger bonds of the molecular moieties.[4,54–58] The fragmentation mechanism of the metastable halogenobenzene cations studied here presents obvious differences with respect to the case of van der Waals complexes, the main one being that IVR is far more complete, with the result that their dissociation is much closer to the statistical limit.[21–26,30,31,35–37,39,59] Quantum mechanically, however, in spite of these differences, both types of vibrational predissociations can be described in terms of metastable states or resonances, excited above the lowest threshold for dissociation. The rate of decay of these quasibound states is controlled by matrix elements, denoted $\langle n|V|\varepsilon\rangle$, between the localized wave function, $|n\rangle$, of a bound state excited above the lowest fragmentation asymptote and an oscillating wave function along the reaction coordinate for the pair of fragments, $|\varepsilon\rangle$. Each particular predissociation process involves a specific coupling operator V and different types of $|n\rangle$ and $|\varepsilon\rangle$ wave functions. However, one common feature is that these matrix elements[54–56,60] are found to decay exponentially as a function of the square root of the kinetic energy, ε, and become already negligible for values of ε smaller than the highest value allowed by conservation of the total energy, E. Although this was first recognized in the study of van der Waals complexes, the fact that, well above the dissociation threshold, the decay widths obey the so-called ''exponential momentum gap law''[54,56] indicates that the propensity rule applies to other predissociation cases as well.

The momentum gap law can be related to the functional form of the constraint, $\sqrt{\varepsilon}$ [Eq. (5.1)] that we have identified in the maximum entropy analysis of the experimental distributions. It implies that the final states with a high value of ε are not produced during the predissociation process and are excluded from the sampling of phase space. Final states with a low value of ε and comparatively more energy in the rotational and vibrational degrees of freedom of the fragments are favored with respect to the prior distribution, which leads to a positive value of the Lagrange multiplier λ_1 in Eq. (5.1). The average kinetic energy of the experimental distribution, $\langle\varepsilon\rangle$, is smaller than the purely statistical one, computed with the prior distribution [Eq. (4.3)].

Information on the statistical nature of the reaction can be obtained via an analysis of the efficiency of phase space sampling. The values obtained for λ_1, DS, and e^{-DS} at $E=E_S$ in the case of bromo- and iodobenzene dissociations, are presented in Table I. The quantity e^{-DS} measures the fraction of phase space sampled by the pair of fragments with respect to the statistical value. Values of the order of 80% are obtained. In these simple bond cleavage reactions, the potential energy curve along the reaction coordinate is thought to increase smoothly without giving rise to an energy barrier and hence to an obvious transition state.[30,31] This has been confirmed by Klippenstein's *ab initio* calculations.[38] The discussion given in part II of this series[39] should be repeated here. Long-range forces between the planar $C_6H_5^+$ fragment and the bromine or iodine atoms presumably contain negligible anisotropic terms and are hardly expected to generate torques. Since the fragments separate with a very small relative velocity, no energy exchange takes place between the receding fragments. Hence, the above-mentioned values are thought to be related to the fraction of phase space accessible to the transition state. This confirms the general consensus about the statistical character of the reaction.

VI. INFLUENCE OF THE INTERNAL ENERGY ON PHASE SPACE SAMPLING

The quantity e^{-DS} is the ratio between the volume of phase space effectively sampled and the total accessible volume. Does the efficiency of phase space exploration increase or decrease as the internal energy E varies?

Right at threshold, the discrimination introduced by the momentum gap law is inoperant because $\varepsilon=0$. Hence, $DS=0$ and $e^{-DS}=1$. Phase space is totally explored when it is reduced to a single cell. As the internal energy increases, the highest possible value of ε increases too, and the ratio between the volume in phase space allowed by the momentum gap law and the total volume in phase space computed from the prior distribution decreases. However, at sufficiently high energies, the momentum gap law can be expected to be less restrictive on purely statistical grounds. The number of states characterized by a dispersion of the entire excess energy E among the subset of internal degrees of freedom increases much more rapidly than those where a significant part of E has flown into the reaction coordinate. In addition to this purely statistical argument, the influence of anharmonicity, and thus the efficiency of IVR, is expected to increase with E, leading to a decrease of λ_1 and thus to an easing of the constraint.

Insight into this problem is provided by modelization. If the density of states $N(E)$ is assumed to increase as the s-th power of the energy, as in the classical approximation,[1,2,4] then the analytical approximation to the KERD is given by

$$P(\varepsilon|E)=[\Gamma(s+2.5)/\Gamma(1.5)\Gamma(s+1)] \times e^{-\lambda_0}E^{-s-1.5}\varepsilon^{1/2}(E-\varepsilon)^s e^{-\lambda_1\varepsilon^{1/2}}, \qquad (6.1)$$

where s is related to the effective number of degrees of freedom.

The classical parametrization of the density of states has well-known shortcomings,[1,2,4] but it provides analytical expressions for the moments of the KERD. The latter can be expressed[61] as generalized hypergeometric series of the dimensionless reduced variable $\lambda_1 E^{1/2}$. Therefore, when either E or λ_1 is equal to zero, these polynomials reduce to their constant term and e^{-DS} reaches its maximum value of one, in agreement with the discussion above. It decreases in an approximately Gaussian way as ${\lambda_1}^2 E$ increases.

These expectations can be compared with the experimental findings reported in Table I where, in the quite narrow energy range investigated, e^{-DS} is observed to undergo a slight decrease as E increases. Although slight, these trends are believed to exceed the error limits.

Equation (6.1) has been applied to the case at hand. The value of s that best fits the rovibrational density of states of the pair of fragments calculated by the Beyer–Swinehardt algorithm is equal to 10. From Table I, a value of 6 $eV^{-1/2}$ was adopted for the parameter λ_1. This leads to values of e^{-DS} equal to 0.85, 0.83, and 0.81 at $E=0.67$, 0.75, and 0.85 eV, respectively. The decrease is not as steep as that observed in the experiment, but the order of magnitude is correct and the trend observed in $C_6H_5Br^+$ is reproduced. To account for that in iodobenzene, a slight decrease of λ_1 as E increases has to be assumed, which is reasonable.

This general behavior seems to be borne out by independent experiments on the vinyl bromide ion, extending over a broader range of internal energies, to be reported in a future paper.[62]

VII. THE DISSOCIATION OF THE CHLOROBENZENE CATION

The KERD of the chlorobenzene cation cannot be fitted by the equations which satisfactorily describe the behavior of the bromo- and iodobenzene ions (Fig. 5). Equation (5.1), together with (2.3), leads to a poor fit of the experimental KERD, as shown in the top panel of Fig. 5. In addition, the averaged surprisal, $\tilde{I}$,

$$\tilde{I}=-\ln\left[\frac{\tilde{P}(\varepsilon)}{\tilde{P}^0(\varepsilon)}\right],$$

where

$$\tilde{P}^0(\varepsilon)=\int_\varepsilon^\infty P^0(\varepsilon|E)T(E)dE,$$

with $\tilde{P}(\varepsilon|E)$ given by Eq. (2.3), is plotted in the lower panel of Fig. 5 as a function of $\sqrt{\varepsilon}$. The averaged surprisal $\tilde{I}$ is a local measure of the relevance of the constraint.[59] Its graph should remain linear in its entire range if $\sqrt{\varepsilon}$ is the only constraint present in the range of values of ε sampled by the experimental distribution. (Average surprisal graphs were also calculated for the bromo- and iodobenzene ions. They are indeed observed to fulfill this condition.) Thus, both panels of Fig. 5 suggest that a second, rather weak component contributes to the KERD for translational energies larger than about 130 meV.

This second component cannot be due to more energetic dissociations induced by collision with the residual gas in the field-free region. Appearance energy measurements conducted by scanning the energy of the ionizing electrons did

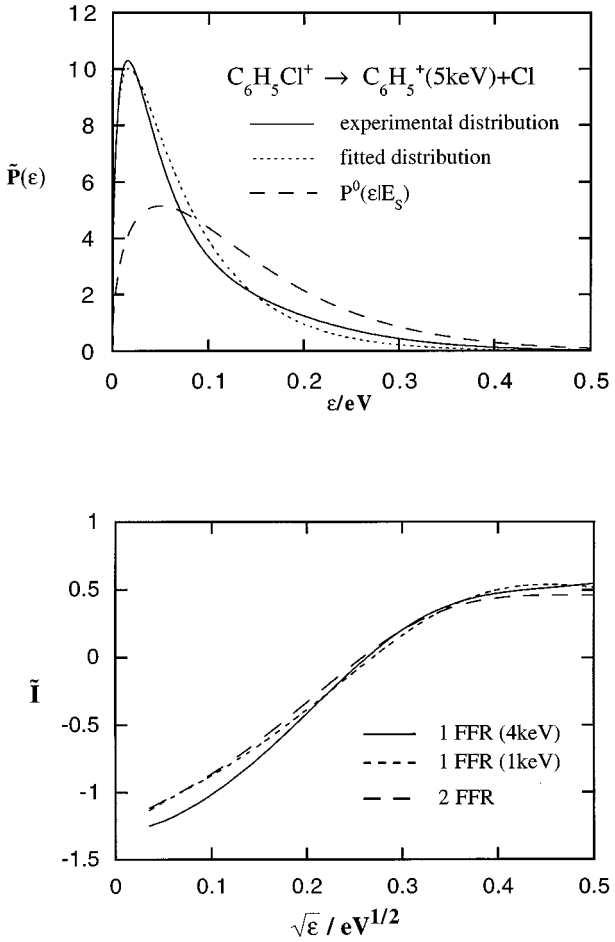

FIG. 5. (Top) solid line: experimental kinetic energy release distribution obtained for the metastable dissociation $C_6H_5Cl^+ \rightarrow C_6H_5^+$ (5 keV)+Cl (first field-free region). The dotted line represents the (unsuccessful) fit to the one-parameter equation (5.1). The prior distribution [Eq. (4.3)] at $E=E_S$ is drawn in dashed lines. (Bottom) nonlinear surprisal plot showing the occurrence of an additional contribution to the KERD.

not show any component below the appearance energy of the $C_6H_5^+$+Cl fragments, as would be expected if collision-induced dissociations were present.

The additional component could be related to either a second dissociation channel or to an additional dynamic constraint. We have systematically investigated these possibilities, using the maximum entropy method.

The introduction of an additional dynamic constraint turned out to be unsuccessful. Neither a modification of the power to which ε is raised, nor trying the vibrational or the rotational energies as constraints, nor simultaneously adopting two constraints, nor allowing the Lagrange parameters to vary with the internal energy led to an improvement of the fit. However, at the higher internal energies sampled for chlorobenzene, the $C_6H_5^+$ ion could conceivably isomerize, thereby leading to a different density of states for the products. We therefore carefully investigated the structure of the $C_6H_5^+$ ion, conducting additional experiments which are described in Sec. VII A below. From these experiments, we conclude that only the phenylium ion is formed when the halogenobenzene cations fragment. In Sec. VII B, we show that for the fragmentation of the $C_6H_5Cl^+$ ions, due to the small value of the spin-orbit coupling, the chlorine atoms can be generated both in their ground and electronic excited states, $^2P_{3/2}$ and $^2P_{1/2}$, while only the ground state, $^2P_{3/2}$, is accessible for the $C_6H_5^+$+Br and $C_6H_5^+$+I fragments. The maximum entropy analysis including this second channel leads to tight fits and indicates that for this second channel the release of the internal energy into the translation degrees of freedom is favored. We then discuss how this could be related to the presence of a barrier along the reaction coordinate.

A. Structure of the $C_6H_5^+$ fragment

In the case of chlorobenzene, the internal energy content of the dissociating parent ion is larger by about 0.5 eV than that of both ionized bromo- and iodobenzene (see Table I). This could open an isomerization pathway for the $C_6H_5^+$ fragment ion, resulting in a different variation of the density of states with internal energy and thus to a different prior distribution. The problem would then have to be treated as a two-exit-channel dissociation.

Tandem mass spectrometric techniques are particularly suitable to probe ionic structures. The major problem which arises to carry out mixture analysis on $C_6H_5^+$ is the absence of well-established structurally pure $C_6H_5^+$ standards. From the available literature,[63,64] it can be concluded that either acetylene condensation reactions at high pressure or ion-assisted dehalogenation reactions of halogenobenzene are thought to lead to a majority of $C_6H_5^+$ ions with the cyclic phenylium structure. *Ab initio* calculations at the self-consistent-field (SCF) 4-31G level,[65] as well as MINDO/3 calculations,[66] show the occurrence of stable open-chain structures which are 0.65–0.7 eV more energetic than the phenylium cation.

According to Cooks *et al.*[63] and to Eyler and Campana,[64] the phenylium structure favors hydrogen loss (leading to a fragment ion at $m/z=76$) and charge stripping (doubly charged ion at $m/z=38.5$). The open-chain structure favors the loss of C_2H_2, leading to a signal at $m/z=51$. As a consequence, the $[m/z=76]/[m/z=51]$, $[m/z=50]/[m/z=51]$, and $[m/z=38.5]/[m/z=37]$ intensity ratios are diagnostic for the cyclic structure.

In order to check for the ionic structure reached in the metastable dissociations considered in this work, a series of collisionally activated dissociation (CAD) experiments were carried out on $C_6H_5^+$ ions produced either in the ion source, or resulting from a metastable decomposition. These experiments have been carried out with the six-sector ($E_1B_1E_2E_3B_2E_4$) AutoSpec 6F mass spectrometer[67] at the University of Mons-Hainaut. This spectrometer has been recently modified by the insertion of an r.f.-only quadrupole collision cell between E_2 and E_3.[68] This instrument has the MS^3 capabilities necessary to perform CAD on ions resulting from a previous metastable dissociation. The MS^3 experiments were carried out as follows. $C_6H_5X^+$ ions were transmitted through the $E_1B_1E_2$ sectors and underwent unimolecular dissociation in the quadrupole cell floated at a voltage similar to the 8 kV accelerating voltage. The so-produced m/z 77 ions were then reaccelerated at ~8 keV, mass-selected by E_3B_2, and subjected to collisional activation with nitrogen in a collision cell between B_2 and

TABLE II. Peak height ratios measured in MIKES-CAD spectra of $C_6H_5^+$ ions.

	$\frac{[m/z=76]}{[m/z=51]}$	$\frac{[m/z=50]}{[m/z=51]}$
C_6H_5Cl	0.20[a]/0.74[b]	0.52[a]/1.13[b]
C_6H_5Br	0.21[a]/0.84[b]	0.56[a]/1.12[b]
C_6H_5I	0.23[a]/0.94[b]	0.50[a]/1.11[b]

[a]The $C_6H_5^+$ ions result from dissociation of $C_6H_5X^+$ in the ion source. The CAD spectra (target gas=O_2) are recorded by scanning E_3.

[b]The $C_6H_5^+$ ions result from metastable dissociation of $C_6H_5X^+$ in the quadrupole located between E_2 and E_3. CAD (target gas=N_2) takes place between B_2 and E_4.

E_4. MIKES spectra were then recorded by scanning E_4. Such a procedure preserves, therefore, the resolution and the sensitivity whatever the mass difference between the $C_6H_5X^+$ and $C_6H_5^+$ ions. The results obtained with the three halogenobenzene precursors for $C_6H_5^+$ ions produced either in the ion source or in a metastable dissociation are summarized in Table II.

The criteria discussed above lead us to the conclusion that the $C_6H_5^+$ ions resulting from a metastable dissociation contain a larger proportion of phenylium ions than those produced in the ion source under higher internal energy conditions. Furthermore, the CAD spectra of $C_6H_5^+$ ions resulting from metastable dissociations with the three different precursors are identical within experimental error, so that these ions have the same structure (or, at least, correspond to the same structural mixture) whatever the selected precursor. A rapid interconversion between cyclic and acyclic structures is not very probable, as CAD allows us to distinguish between different ways of producing $C_6H_5^+$. As the $[m/z=50]/[m/z=51]$ ratio is even larger than the ratio measured by Eyler and Campana in the case of ion-assisted dehalogenation of fluorobenzene, we may conclude that pure phenylium ions result from the dissociation of the three investigated halogenobenzene cations. At this point, it must also be mentioned that appearance energy measurements of metastably produced $C_6H_5^+$ from the three precursors are compatible with a unique structure for the three cases. All these observations confirm the high activation barrier for cycle opening.[66] With ionized chlorobenzene undergoing metastable decomposition, the internal energy content is of the order of 1.3 eV for an accelerating voltage of 8 kV: this provides us with a lower limit for the isomerization barrier. These experiments lead us to the conclusion that only the phenylium ion structure has to be considered in our maximum entropy analysis of the kinetic energy release distributions of chloro-, bromo-, and iodobenzene cations.

B. The composite nature of the reaction

An attempt was then made to interpret the KERD as resulting from a two-channel process, involving electronic excitation. A correlation diagram between the electronic states of $C_6H_5Cl^+$ determined by photoelectron spectroscopy and those of its fragments is presented in Fig. 6 to obtain a schematic set of adiabatic potential energy curves.

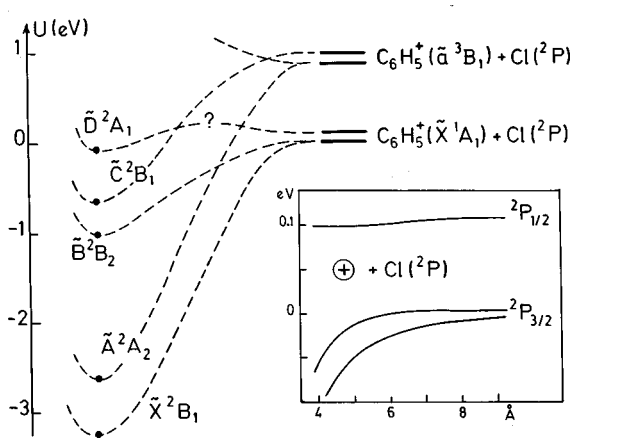

FIG. 6. Schematic set of potential energy curves for the $C_6H_5Cl^+ \rightarrow C_6H_5^+ + Cl$ reaction. Experimental data about the position of electronic states of the ion and about the dissociation asymptotes are represented by heavy dots and full lines, respectively. The dashed lines represent mere correlations. Inset: results of *ab initio* calculations (see text) on the action of a point charge on a chlorine atom.

The production of a significant amount of $C_6H_5^+$ in its excited triplet state can be discarded by a statistical argument based on the substantial energy gap ($\approx$0.8–1.0 eV)[69–71] between the ground and excited states. At values of the internal energy close to E_S, the density of the vibrational-rotational states of $C_6H_5^+$ is much smaller (by at least three or four orders of magnitude) in the triplet than in the ground singlet state.

However, very good results were obtained when the generation of the Cl atom in both of its states, $^2P_{3/2}$ and $^2P_{1/2}$, was taken into account. In contradistinction to the Br and I atoms, the small value of the spin-orbit splitting in the Cl atom (0.11 eV) with respect to the average internal energy makes it statistically possible to generate both states in competition. This higher threshold energy channel induces a second component in the kinetic energy distribution. Since the available information is the kinetic energy distribution of the pair of fragments irrespective of the electronic state of the chlorine atom, a ''synthetic'' analysis[72,73] of the experimental results was carried out. It was assumed that each rovibrational state of the phenyl cation can be accompanied by either a ground or an excited chlorine atom. This leads to the following expression for the kinetic energy distribution, where E_{SO} is the energy difference between the two electronic states of the chlorine atom, resulting from the spin-orbit coupling (E_{SO}=0.11 eV),

$$P(\varepsilon|E)=C(E)[pP_1(\varepsilon|E)+(1-p)P_2(\varepsilon|E)] \quad \text{for } E\geqslant E_{SO} \text{ and } \varepsilon\leqslant E-E_{SO},$$
$$P(\varepsilon|E)=C(E)P_1(\varepsilon|E) \quad \text{otherwise,} \tag{7.1}$$

p and $(1-p)$ define the branching ratio between the two channels. $C(E)$ is the normalization factor. Using $\varepsilon^{1/2}$ as a single constraint in the two channels leads to the following equations for $P_1(\varepsilon|E)$ and $P_2(\varepsilon|E)$:

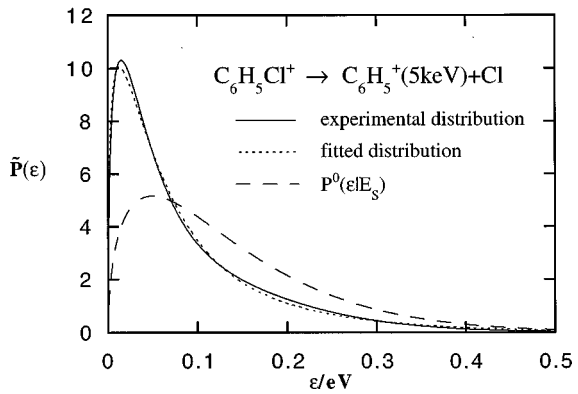

FIG. 7. Solid line: experimental kinetic energy release distribution obtained for the metastable dissociation $C_6H_5Cl^+ \rightarrow C_6H_5^+$ (5 keV)+Cl (first field-free region). Dotted line: fit including two Lagrange parameters [Eqs. (7.1) and (7.2)]. Dashed lines: prior distribution [Eq. (4.3)] at $E=E_S$.

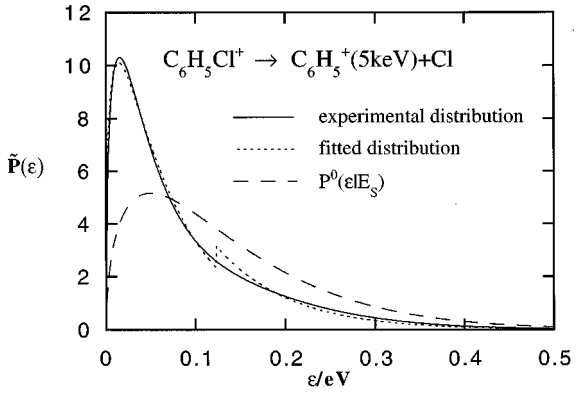

FIG. 8. Solid line: experimental kinetic energy release distribution obtained for the metastable dissociation $C_6H_5Cl^+ \rightarrow C_6H_5^+$ (5 keV)+Cl (first field-free region). Dotted line: fit assuming the existence of a potential energy barrier [Eqs. (7.3) and (7.4)]. Dashed lines: prior distribution [Eq. (4.3)] at $E=E_S$.

$$P_1(\varepsilon|E)=P^0(\varepsilon|E)\exp(-\lambda_0-\lambda_1\varepsilon^{1/2}),$$
$$P_2(\varepsilon|E)=P^0(\varepsilon|E-E_{SO})\exp(-\lambda_0'-\lambda_1'\varepsilon^{1/2}), \tag{7.2}$$

where the primed Lagrange parameters λ_0' and λ_1' refer to the second channel.

The experimental results have been fitted to Eqs. (7.1) and (7.2) [taking into account the averaging over the collection efficiency $T(E)$ as in Eq. (2.3)]. The nice fit shown in Fig. 7 leads to the following interpretation. Two independent reaction channels are open in the fragmentation of $C_6H_5Cl^+$. The main contribution ($p=0.85\pm0.03$) is very similar to that observed in $C_6H_5Br^+$ and in $C_6H_5I^+$. It leads to a halogen atom in its $^2P_{3/2}$ state with a positive λ_1 Lagrange parameter (implying a release of kinetic energy less than the statistical estimate). The observed value for e^{-DS} ($\approx$80%) is quite similar to that found in the case of $C_6H_5Br^+$ and of $C_6H_5I^+$.

In addition, a weaker contribution is also observed. It is characterized by a negative Lagrange parameter λ_1', whose absolute value has the same order of magnitude as λ_1 (and thus is well outside the uncertainties), but which is now negative. The negative sign indicates a release of translational energy larger than the statistical expectation. Therefore, unlike the component leading to the Cl atom in its ground electronic state, the second component is not controlled by the momentum gap law (which disfavors the high values of the kinetic energy) but by a process which favors the release of the internal energy to the relative translational motion of the fragments.

Such a process could be due to the presence of a small barrier along the reaction coordinate, if the barrier energy is preferentially converted into relative translational energy of the fragments. To estimate the height of this barrier, we made the further assumption that the energy of the barrier (denoted Δ) is completely converted into translational energy of the fragments. Equations (7.1) and (7.2) can then be replaced by the following ones, in which λ_1' has been set equal to zero and in which the internal energy averaging is explicitly introduced,

$$\tilde{P}(\varepsilon)=p\int_{\varepsilon}^{\infty}T(E)C(E)P^0(\varepsilon|E)\exp(-\lambda_0-\lambda_1\varepsilon^{1/2})dE$$
$$+(1-p)\int_{\varepsilon+\Delta}^{\infty}T(E)C(E)P^0(\varepsilon|E-E_{SO})dE, \tag{7.3}$$

valid when $E\geqslant E_{SO}+\Delta$ and when $\Delta\leqslant\varepsilon\leqslant E-E_{SO}$, and

$$\tilde{P}(\varepsilon)=\int_{\varepsilon}^{\infty}T(E)P^0(\varepsilon|E)\exp(-\lambda_0-\lambda_1\varepsilon^{1/2})dE, \tag{7.4}$$

when $E\leqslant E_{SO}+\Delta$ or when $\Delta\geqslant\varepsilon\geqslant E-E_{SO}$.

The fit to the experimental data is shown in Fig. 8, while the values of λ_1, DS, and e^{-DS} obtained for the first channel are given in Table I. Δ can be estimated to be about 0.12 eV. A value of 0.9 ± 0.03 was obtained for the branching ratio p. This is in good agreement with the branching ratio obtained from the fit to Eqs. (7.1) and (7.2). The discontinuity observed when $\varepsilon\approx\Delta$ has little physical significance. It results from our neglect of tunneling.

The existence of a small barrier along the reaction path of state $\tilde{D}$ is predicted by *ab initio* calculations carried out by Klippenstein.[38] It is compatible with the theory of long-range forces. The interaction between a fluorine atom and a positive point charge has been predicted by Gentry and Giese[74] to generate two attractive potential energy curves correlating with the $^2P_{3/2}$ state and one curve with a hump correlating with the $^2P_{1/2}$ state of *F*. The same model was applied to the chlorine atom. A series of *ab initio* calculations of increasing accuracy were carried out using Dunning's correlation consistent basis sets[75] to determine its quadrupole moment and its anisotropic polarizabilities. The best calculations[76] [UMP2/AUG-cc-pVQZ (80 basis functions) and B3LYP/AUG-cc-pV5Z (131 basis functions)] led to nearly identical sets of potential energy curves, reported in the inset of Fig. 6. Two attractive curves are found to connect the $^2P_{3/2}$ state of Cl to the $\tilde{X}\,^2B_1$ and $\tilde{B}\,^2B_2$ states of $C_6H_5Cl^+$ without any barrier. A third one connects the $^2P_{1/2}$ state of Cl to $\tilde{D}\,^2A_1$. Its remarkably horizontal shape (together with Klippen-

stein's results) implies that the postulated barrier is determined by higher terms in the multipole expansion and by incipient exchange terms.

Coming back to the reaction mechanism, it should be remembered that one is studying a process with a lifetime of the order of a few microseconds. Hence, it would be unreasonable to assume that the population of state $\tilde{D}$ has escaped efficient internal conversions for which a lifetime of the order of 10^{-13} s is usually proposed.[77] Instead, it can be assumed that the entire population has relaxed to the ground $\tilde{X}\,^2B_1$ electronic state. Then, during the final stretch of the reaction coordinate that leads to products, a small fraction $[(1-p)\approx 0.1]$ of the population of the ground state $\tilde{X}$ undergoes a transition back to state $\tilde{D}$. This is made plausible by noting the existence of an avoided crossing along the reaction path between states $\tilde{X}$ and $\tilde{C}$. The ground electronic state $\tilde{X}\,^2B_1$ has five π electrons in its electronic shell and diabatically correlates to the triplet state of the $C_6H_5^+$ fragment (which has a $\pi^5 n^1$ configuration), not to its ground singlet state (which has a π^6 configuration). Conversely, the diabatic correlation for the π^6 configuration connects state $\tilde{C}$ with the lowest dissociation asymptote. The resulting nonadiabatic interaction could be responsible for a transfer of population from state $\tilde{X}$ to $\tilde{C}$, followed by a predissociation of state $\tilde{C}$ by $\tilde{D}$ via a conical intersection. It should furthermore be noted that the electronic configurations of the three states $\tilde{X}$, $\tilde{C}$, and $\tilde{D}$ are singly excited with respect to each other. This circumstance is compatible with a substantial interaction.

In the case of $C_6H_5Br^+$ and $C_6H_5I^+$, the back transition to state $\tilde{D}$ is highly improbable because of the large magnitude of the spin-orbit splitting in the bromine and iodine atoms.

VIII. CONCLUDING REMARKS

Three conclusions can be drawn from the present analysis of the unimolecular dissociation of the halogenobenzene ions.

(1) The theoretical analysis of the KERD is carried out at an infinite value of the reaction coordinate. In principle, it is noncommittal concerning the properties and even the existence of a transition state at a finite value of the reaction coordinate. However, information on the reaction mechanism can be obtained by identifying the nature of the informative variable responsible for its nonstatistical character. The functional form of the relevant constraint, $\varepsilon^{1/2}$, can be related to the theory of vibrational predissociation. Quantum mechanically, the predissociation process is described by the decay of resonant states, which are quasibound states coupled to the fragmentation channels. Their dissociation rates follow the ''momentum gap law''[54–56,60] and involve matrix elements which decay exponentially with the square root of the relative kinetic energy of the fragments. The exploration of phase space is systematically hindered for high values of the relative translational momentum of the fragments, leading to a value of the fraction of the sampled phase space volume smaller than the one expected on grounds of the prior distribution.

(2) Not surprisingly, the family of the halogenobenzene cations is homogeneous and the values obtained for the entropy deficiency and phase space sampling are very similar. The analysis carried out here and the obtained values for the entropy deficiency concern the energy partitioning between the reaction coordinate and the set of the remaining coordinates (which may be denoted as a bath, although no thermal equilibrium is implied). It can be concluded that this partitioning is nearly statistical, but not quite: less translational energy is channeled into the reaction coordinate than the statistical estimate. Unfortunately, as we are not able to extract more than one constraint from these relatively smooth KERD, no conclusion can be derived concerning the energy partitioning within the bath.

(3) The method is able to supply further information on the reaction mechanism by demonstrating the composite nature of the fragmentation of $C_6H_5Cl^+$. The major dissociation channel (90%) leads to the chlorine atom in its ground electronic state, $^2P_{3/2}$, and displays a behavior very similar to the other halogenobenzene cations. For the additional minor channel (10%), the kinetic energy released on the fragments is larger than the prior estimate. Our data suggest the probable existence of a small barrier ($\approx$0.12 eV) along this reaction path, which leads to $C_6H_5^+ + Cl(^2P_{1/2})$. The appearance of this second component may be related to earlier findings[24,37] that the chlorobenzene ion decomposition appears to require a nontotally loose complex.

ACKNOWLEDGMENTS

The authors thank Professor R. D. Levine for helpful discussions on the maximum entropy formalism and Dr. M. Godefroid for his advice on the calculation of atomic properties. P.U. is grateful to the F.R.I.A. for a research fellowship. This work has been supported by the ''Fonds National de la Recherche Scientifique,'' by the ''Fonds de la Recherche Fondamentale Collective'' and by research grants from the University of Liège. B.L. and F.R. thank the FNRS (Belgium) for a research associateship.

[1] W. Forst, *Theory of Unimolecular Reactions* (Academic, New York, 1973).
[2] R. G. Gilbert and S. C. Smith, *Theory of Unimolecular and Recombination Reactions* (Blackwell Scientific, Oxford, 1990).
[3] J. C. Lorquet, Mass Spectrom. Rev. **13**, 233 (1994).
[4] T. Baer and W. L. Hase, *Unimolecular Reaction Dynamics. Theory and Experiments* (Oxford University Press, New York, 1996).
[5] C. E. Klots, J. Phys. Chem. **75**, 1526 (1971).
[6] C. E. Klots, Z. Naturforsch. A **27**, 553 (1972).
[7] M. Quack and J. Troe, Ber. Bunsenges. Phys. Chem. **78**, 240 (1974).
[8] C. Lifshitz, Adv. Mass Spectrom. **7A**, 3 (1978).
[9] W. J. Chesnavich and M. T. Bowers, in *Gas Phase Ion Chemistry*, edited by M. T. Bowers (Academic, New York, 1979).
[10] C. Lifshitz, J. Phys. Chem. **87**, 2304 (1983).
[11] C. Lifshitz, Adv. Mass Spectrom. **11A**, 713 (1989).
[12] C. Lifshitz, Adv. Mass Spectrom. **12**, 315 (1992).
[13] R. D. Levine, Ber. Bunsenges. Phys. Chem. **78**, 113 (1974).
[14] T. Sewell, D. L. Thompson, and R. D. Levine, J. Phys. Chem. **96**, 8006 (1992).

[15] E. T. Jaynes, Phys. Rev. **106**, 620 (1957).
[16] R. D. Levine and R. B. Bernstein, in *Dynamics of Molecular Collisions, Part B*, edited by W. H. Miller (Plenum, New York, 1976).
[17] R. D. Levine and J. L. Kinsey, in *Atom-Molecule Collision Theory. A Guide for the Experimentalist*, edited by R. B. Bernstein (Plenum, New York, 1979).
[18] R. D. Levine, Adv. Chem. Phys. **47**, 239 (1981).
[19] R. D. Levine, in *Theory of Chemical Reaction Dynamics*, edited by M. Baer (CRC, Boca Raton, Fl, 1985).
[20] R. D. Levine and R. B. Bernstein, *Molecular Reaction Dynamics and Chemical Reactivity* (Oxford University Press, New York, 1987).
[21] T. Baer, B. P. Tsai, D. Smith, and P. T. Murray, J. Chem. Phys. **64**, 2460 (1976).
[22] H. M. Rosenstock and R. Stockbauer, J. Chem. Phys. **71**, 3708 (1979).
[23] H. M. Rosenstock, R. Stockbauer, and A. C. Parr, J. Chem. Phys. **73**, 773 (1980).
[24] S. T. Pratt and W. A. Chupka, Chem. Phys. **62**, 153 (1981).
[25] T. Baer and R. Kury, Chem. Phys. Lett. **92**, 659 (1982).
[26] J. Dannacher, H. M. Rosenstock, R. Buff, A. C. Parr, R. L. Stockbauer, R. Bombach, and J.-P. Stadelmann, Chem. Phys. **75**, 23 (1983).
[27] W. A. Brand, J. Stocklöv, and H. J. Walther, Int. J. Mass Spectrom. Ion Processes **59**, 1 (1984).
[28] P. C. Burgers and J. L. Holmes, Int. J. Mass Spectrom. Ion Processes **58**, 15 (1984).
[29] J. L. Durant, D. M. Rider, S. L. Anderson, F. D. Proch, and R. N. Zare, J. Chem. Phys. **80**, 1817 (1984).
[30] Y. Malinovich, R. Arakawa, G. Haase, and C. Lifshitz, J. Phys. Chem. **89**, 2253 (1985).
[31] Y. Malinovich and C. Lifshitz, J. Phys. Chem. **90**, 2200 (1986).
[32] R. C. Dunbar, J. Phys. Chem. **91**, 2801 (1987).
[33] R. J. Stanley, M. Cook, and A. W. Castleman, J. Phys. Chem. **94**, 3668 (1990).
[34] X. Ripoche, I. Dimicoli, and R. Botter, Int. J. Mass Spectrom. Ion Processes **107**, 165 (1991).
[35] C. Lifshitz, F. Louage, V. Aviyente, and K. Song, J. Phys. Chem. **95**, 9298 (1991).
[36] Y. H. Yim and M. S. Kim, J. Phys. Chem. **97**, 12122 (1993).
[37] Y. H. Yim and M. S. Kim, J. Phys. Chem. **98**, 5201 (1994).
[38] S. J. Klippenstein, Int. J. Mass Spectrom. Ion Processes **167/168**, 235 (1997).
[39] P. Urbain, F. Remacle, B. Leyh, and J. C. Lorquet, J. Phys. Chem. **100**, 8003 (1996).
[40] M. Barber and R. M. Elliot, *12th Annual Conference on Mass Spectrometry and Allied Topics*, Montreal, 1964.
[41] R. K. Boyd and J. H. Beynon, Org. Mass Spectrom. **12**, 163 (1977).
[42] S. Harakawa, M. Yoshioka, and T. Sugiura, Int. J. Mass Spectrom. Ion Processes **87**, 309 (1989).
[43] J. L. Holmes and A. D. Osborne, Int. J. Mass Spectrom. Ion Phys. **23**, 189 (1977).
[44] R. G. Cooks, J. H. Beynon, R. M. Caprioli, and G. R. Lester, *Metastable Ions* (Elsevier, Amsterdam, 1973).
[45] J. H. Beynon, A. E. Fontaine, and G. R. Lester, Int. J. Mass Spectrom. Ion Phys. **8**, 341 (1972).
[46] A. Kafri, Chem. Phys. **13**, 309 (1976).
[47] R. D. Levine and R. B. Bernstein, Faraday Discuss. Chem. Soc. **55**, 100 (1973).
[48] R. C. Tolman, *The Principles of Statistical Mechanics* (Oxford University Press, London, 1938).
[49] P. Pechukas and J. C. Light, J. Chem. Phys. **42**, 3281 (1965).
[50] C. E. Klots, J. Chem. Phys. **64**, 4269 (1976).
[51] S. E. Stein and B. S. Rabinovitch, J. Chem. Phys. **58**, 2438 (1973).
[52] F. Iachello and R. D. Levine, Europhys. Lett. **4**, 389 (1987).
[53] R. D. Levine, Adv. Chem. Phys. **70**, 53 (1988).
[54] G. E. Ewing, J. Chem. Phys. **71**, 3143 (1979).
[55] G. E. Ewing, J. Chem. Phys. **72**, 2096 (1980).
[56] J. A. Beswick and J. Jortner, Adv. Chem. Phys. **47**, 363 (1981).
[57] *Dynamics of Polyatomic van der Waals Complexes*, edited by N. Halberstadt and K. C. Janda (Plenum, New York, 1990).
[58] *Mode Selective Chemistry*, edited by J. Jortner, R. D. Levine, and B. Pullman (Kluwer, Dordrecht, 1991).
[59] P. Urbain, B. Leyh, F. Remacle, and J. C. Lorquet, Int. J. Mass Spectrom. **178** (1998).
[60] M. Desouter-Lecomte, J. Liévin, and V. Brems, J. Chem. Phys. **103**, 4524 (1995).
[61] I. S. Gradshteyn and I. M. Ryzhik, *Table of Integrals, Series, and Products* (Academic, New York, 1965).
[62] A. Hoxha, B. Leyh, and R. Locht, work in progress.
[63] R. G. Cooks, J. H. Beynon, and J. F. Litton, Org. Mass Spectrom. **10**, 503 (1975).
[64] J. R. Eyler and J. E. Campana, Int. J. Mass Spectrom. Ion Processes **55**, 171 (1983).
[65] J. D. Dill, P. V. R. Schleyer, J. S. Binkley, R. Seeger, J. A. Pople, and E. Haselbach, J. Am. Chem. Soc. **98**, 5428 (1976).
[66] M. Tasaka, M. Ogata, and H. Ichikawa, J. Am. Chem. Soc. **103**, 1885 (1981).
[67] R. H. Bateman, J. Brown, M. Lefevere, R. Flammang, and Y. V. Haverbeke, Int. J. Mass Spectrom. Ion Processes **115**, 205 (1992).
[68] R. Flammang, Y. V. Haverbeke, C. Braybrook, and J. Brown, Rapid Commun. Mass Spectrom. **9**, 795 (1995).
[69] J. Hrusak, D. Schröder, and S. Iwata, J. Chem. Phys. **106**, 7541 (1997).
[70] A. Nicolaides, D. M. Smith, F. Jensen, and L. Radom, J. Am. Chem. Soc. **119**, 8083 (1997).
[71] J. N. Harvey, M. Aschi, H. Schwarz, and W. Koch, Theor. Chem. Acc. **99**, 95 (1998).
[72] U. Dinur, R. Kosloff, R. D. Levine, and M. J. Berry, Chem. Phys. Lett. **34**, 199 (1975).
[73] Y. Ozaki, T. Kondow, and K. Kuchitsu, Chem. Phys. **77**, 223 (1983).
[74] W. R. Gentry and C. F. Giese, J. Chem. Phys. **67**, 2355 (1977).
[75] D. E. Woon and J. T. H. Dunning, J. Chem. Phys. **98**, 1358 (1993).
[76] M. J. Frisch, G. W. Trucks, H. B. Schlegel, P. M. W. Gill, B. G. Johnson, M. A. Robb, J. R. Cheeseman, T. Keith, G. A. Petersson, J. A. Montgomery, K. Raghavachari, M. A. Al-Laham, V. G. Zakrzewski, J. V. Ortiz, J. B. Foresman, C. Y. Peng, P. Y. Ayala, W. Chen, M. W. Wong, J. L. Andres, E. S. Replogle, R. Gomperts, R. L. Martin, D. J. Fox, J. S. Binkley, D. J. Defrees, J. Baker, J. P. Stewart, M. Head-Gordon, C. Gonzalez, and J. A. Pople, GAUSSIAN 94, Revision B.3 (Gaussian, Inc., Pittsburgh, 1995).
[77] H. Köppel, W. Domcke, and L. S. Cederbaum, Adv. Chem. Phys. **57**, 59 (1984).